ECS Journal of Solid State Science and Technology, **1** (5) Q106-Q109 (2012)
2162-8769/2012/1(5)/Q106/4/$28.00 © The Electrochemical Society

Crystallized Indium-Tin Oxide (ITO) Thin Films Grown at Low Temperature onto Flexible Polymer Substrates

Hyung-Jin Choi,[a] Soon-Gil Yoon,[a,*,z] Ju-Ho Lee,[b] and Jeong-Yong Lee[c]

[a]*Department of Materials Engineering, Chungnam National University, Daeduk Science Town, Daejeon 305–764, Korea*
[b]*Korea Reliability Technology Research Center, Korea Electronics Technology Institute (KETI), Seongnam 463–816, Korea*
[c]*Department of Materials Science, Korea Advanced Institute of Science and Technology, Daejeon 305–701, Korea*

Facial off-axis sputtering was used to crystallize in situ-grown ITO films onto a polyethylene terephthalate (PET) substrate at 120°C. The process caused no mechanical damage to the substrate. The 100-nm-thick crystalline ITO films showed a resistivity of about 4.2×10^{-4} Ω-cm and a transmittance of about 83% at a wavelength of 550 nm. The crystallized ITO films showed an improved mechanical durability compared with the amorphous ITO films. The integration of a 30-nm-thick amorphous SiO_2 layer onto ITO/PET maintains the resistivity of the ITO films and exhibits an improvement in the transmittance of about 86% compared with the crystalline ITO films. The amorphous SiO_2 layer did not adversely affect the mechanical durability of either the crystalline ITO or the amorphous ITO films grown onto the PET. The crystalline ITO films on flexible polymer substrates are indispensable for the mechanical durability of flexible touch screens.
© 2012 The Electrochemical Society. [DOI: 10.1149/2.016205jss] All rights reserved.

Manuscript submitted June 13, 2012; revised manuscript received August 20, 2012. Published September 20, 2012.

ITO is the transparent conductor of choice for most display applications due to its superior combination of environmental stability, relatively low electrical resistivity and high transparency. Additionally, the optimization of ITO thin films is a crucial part of the development of new technologies, i.e., transparent bottom contact electrodes for electrochromic displays, organic light-emitting diodes (OLEDs), and organic photovoltaic cells (OPVs).[1,2] Reported values of resistivity of ITO thin films obtained using various deposition techniques are in the range from 6.8 to 3×10^{-4} Ω-cm with a transparency greater than 85% in the visible range.[3–9] The devices using glass substrates are somewhat heavy and very fragile, while those of polymeric substrates are significantly lighter and more flexible. Thus, for transparent conducting applications, particularly OLEDs and photovoltaic components, there has been an increased demand for ITO films that are deposited onto polymeric substrates instead of conventional glass substrates.

Various deposition techniques have been used to prepare high-quality ITO films including electron beam evaporation,[10] ion beam assisted deposition,[11] pulsed laser deposition,[12] nano-cluster deposition,[13,14] and direct current/radio frequency(dc/rf) magnetron sputtering.[8,15,16] Among these deposition methods, sputtering deposition is widely used for ITO film deposition, because it can easily place uniform film over a large area. However, using conventional dc/rf magnetron sputtering for deposition of the crystallized ITO films onto a polymer substrate is difficult because the crystallization of the ITO film requires a high temperature (≥ 250°C). Although the polymer substrates placed in a dc/rf plasma atmosphere were maintained at a low substrate temperature for crystallization, polymer substrates were severely damaged by both the plasma atmosphere and the substrate temperature. However, facial off-axis sputtering can suppress the high energy particle bombardment to the substrate by secondary electrons and negative oxygen ions.[17] Therefore, facial off-axis sputtering seems to be useful to realize a high deposition rate of the oxide films on a plastic substrate, since deposition at a much higher sputtering voltage can be utilized with facial off-axis sputtering than with magnetron sputtering.[18]

The crystallized ITO films showed a higher transmittance and lower resistivity than amorphous films.[8] Although the crystallized ITO films have many advantages, deposition of high-quality crystallized ITO films onto a polymer substrate has not been reported.

In the present study, the crystallized ITO films were prepared in situ and placed onto the PET substrate using facial off-axis sputtering. The resistivity and the transmittance of the crystallized ITO films were compared with the amorphous ITO films using an investigation of the structural properties. For touch-screen applications, the mechanical endurance of the crystallized ITO films was also investigated and was compared with the amorphous films. In order to reduce the light reflectivity of the ITO films, SiO_2 layers of various thicknesses were integrated onto the ITO films and the SiO_2/ITO/PET structures were characterized for transmittance, resistivity, and mechanical durability.

Experimental

Prior to the deposition of ITO films, PET substrates were cleaned by sequential ultrasonic rinses in detergent solution, acetone, distilled acetone, de-ionized water, and then dried in high-purity nitrogen. The ITO films were deposited in a chamber with a facial off-axis rf sputtering system using argon as the sputtering gas. A schematic diagram of facial off-axis sputtering appears in previous work.[18,19] The sputtering target was a ceramic In_2O_3-SnO_2 2 inch-disk (Sn 10 wt%) with 99.99% purity. The 2 ITO targets were faced at a distance of 8 cm. The PET substrates were mounted onto a holder with a diameter of 20 cm and were located 9 cm from the source, which was apart from the plasma. The deposition temperature used to obtain the crystallized ITO films was maintained at 120°C under the following conditions: rf power, 100 W; argon flow rate, 10 sccm (standard cc min^{-1}); and, working pressure, 1.3×10^{-1} Pa. A substrate temperature of 120°C was the maximum temperature chosen that would guarantee the thermal stability of the PET substrate. The precise substrate temperature was measured using a thermocouple mounted on the sample holder, and the substrate holder was rotated for the homogeneous deposition of the films. The film thickness was varied from 100 to 300 nm and the thickness of the ITO films grown onto the PET substrate was determined using an α-step profiler (Tencor 500). The thickness of the films was compared with that of the ITO films deposited onto a Si (001) substrate (using SEM cross-sectional image). The amorphous ITO films were deposited under the same conditions, but without the heating of the substrate that was used for the deposition of the crystallized films.

For the measurement of ITO film properties, the structural properties of the crystallized and the amorphous films were analyzed with X-ray diffraction (XRD, REGAKU D/MAX-RC) using CuK_α radiation and a nickel filter, and a transmission electron microscope (TEM). The surface roughness of the films was investigated using atomic force microscopy (AFM, Auto Probe CP). Sheet resistance of the samples was measured using a four-point probe method. The optical properties were measured using an HP 8453 UV-VIS spectrophotometer. To enhance the electrical properties of the crystallized ITO films, amorphous SiO_2 films of various thicknesses were deposited onto ITO/PET using *on-axis* rf sputtering (using 3 inch-diameter SiO_2 ceramic target)

*Electrochemical Society Active Member.
zE-mail: sgyoon@cnu.ac.kr

Downloaded on 2013-09-11 to IP 143.248.118.122 address. Redistribution subject to ECS license or copyright; see ecsdl.org/site/terms_use

under the following deposition conditions: rf power, 100 W; distance between target and substrate, 10 cm; working pressure, 1.3×10^{-1} Pa; argon flow rate, 20 sccm; and, O_2, 2 sccm. For touch-screen applications of the ITO/PET and SiO_2/ITO/PET films, long-term mechanical endurance was required for impact conditions that would endure finger touch, 1.65×10^{-3} N · m, and pen touch, 3.75×10^{-3} N · m.[20] To test the mechanical endurance, a ZrO_2 ceramic ball (weight: 18.4 g) that was 1.1 cm in diameter and 3 cm in height was repeatedly dropped onto the ITO/PET and SiO_2/ITO/PET films from a height of 15 cm. The impact conditions of the mechanical test using the ZrO_2 ceramic ball were approximately 2.76×10^{-3} N · m, which placed them within the range of both finger and pen touches.

Results and Discussion

Figure 1a shows the XRD patterns of ITO films of various thicknesses grown onto a PET substrate at room temperature and 120°C. The films grown at room temperature were approximately 100 nm in thickness, and indicated the amorphous phase of the ITO film by showing only peaks that exhibited the PET substrate. On the other hand, films grown at 120°C had various peaks at (222), (400), and (440), which showed a polycrystalline nature. The peak intensities of the ITO films increased with increasing thickness. The crystalline size of the films was calculated using the Scherrer formula[21] and the full-width-half-maximum (FWHM) values (θ-2θ scan). The grain size varied from 25 to 28 nm with thicknesses that ranged from 100–300 nm and a root mean square (rms) roughness that increased in a linear fashion from 3.2 to 5.2 nm. A visual reference to the crystallinity of the films is shown in Fig. 1b and 1c, which depicts the TEM images and selective area diffraction patterns (SADP) of the ITO films grown onto an Si (001) substrate at room temperature and at 120°C, respectively. In the present study, because the crystallinity of the films grown onto a PET polymer substrate is impossible to evaluate using the TEM technique, ITO films grown onto an Si (001) substrate instead of a PET substrate were used. The crystalline nature of an Si substrate may ultimately lead to better crystallinity of the ITO films grown at 120°C, compared with that on PET. However, because the crystallinity of the ITO films grown onto PET at 120°C was clearly confirmed by the XRD patterns (Fig. 1a), the analysis of the crystallinity of the ITO films grown onto an Si substrate using TEM has value. As shown in Fig. 1b, films deposited at room temperature showed an amorphous structure from the SADP, while the cross-sectional image of the films grown at 120°C (see Fig. 1c) showed a crystalline phase with (222), (400), and (440) planes from the SADP (see the right image of Fig. 1c). These results were consistent with the XRD results shown in Fig. 1a. It was interesting to investigate why the facial off-axis sputtering was more favorable than the conventional on-axis sputtering for the deposition of the crystallized ITO films at the same deposition temperature of 120°C and the same power of 100 W. In the case of conventional on-axis sputtering, because the PET substrate was severely damaged by thermal energy and plasma, the deposition of the ITO was performed onto the Si (001) substrate instead of the PET. Figures 1d and 1e show the XRD patterns of the ITO films deposited onto the Si (001) substrate by facial off-axis sputtering and conventional on-axis sputtering, respectively. In Figs. 1d and 1e, the peak of the Si (001) substrate at $2\theta = 33°$ was removed for a clear identification of the ITO peaks. As shown in Fig. 1d, ITO films grown by facial off-axis sputtering showed a well-crystallized nature and exhibited sharp peaks in the (222), (400) and (440) planes, while ITO films grown by conventional on-axis sputtering (see Fig. 1e) showed broad peaks in the (222), (400), and (440) planes. From calculation using the Scherrer formula, the particle sizes of the ITO films were about 29 nm (facial off-axis sputtering) and 14 nm (on-axis sputtering). The resistivity of the ITO films was approximately 6.4×10^{-4} Ω-cm (off-axis) and 1.5×10^{-3} Ω-cm (on-axis). Compared with the conventional on-axis sputtering, ITO films grown by facial off-axis sputtering have much smaller compressive stress, which can be attributed to the fact that bombardment by high- energy particles (in the case of the on-axis sputtering) is completely suppressed in facial off-axis sputtering.[18] Higher compressive stress existing in the films plays a critical role in suppression of the crystallinity and in the grain growth of the ITO films.

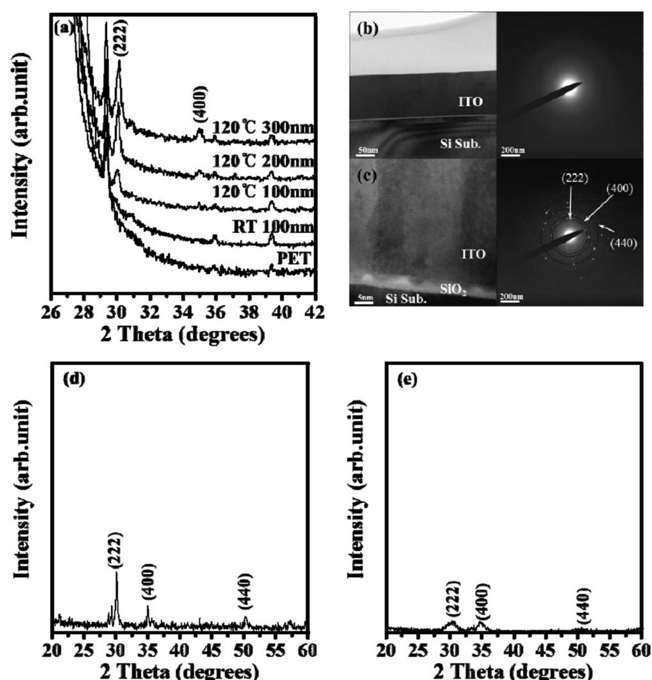

Figure 1. (a) XRD patterns of ITO films of various thicknesses grown onto the PET at room temperature and 120°C. Cross-sectional TEM image (left figure) and the selected area diffraction pattern (right figure) of (b) the amorphous and (c) the crystalline ITO films grown onto Si (001) substrates. XRD patterns of the 100-nm-thick ITO films grown at 120°C and an rf power of 100 W onto a Si (001) substrate using (d) facial off-axis sputtering and (e) conventional on-axis sputtering.

Figures 2a and 2b show the variations in sheet resistance and the transmission of the ITO films, respectively, as a function of thickness. As shown in Fig. 2a, the sheet resistance and the resistivity of the amorphous ITO films deposited at room temperature were approximately 200 Ω/sq. and 2×10^{-3} Ω-cm, respectively. On the other hand, sheet resistance decreased with increasing thickness of the crystallized ITO films, indicating a constant resistivity of about 6×10^{-4} Ω-cm. The resistivity of the crystallized ITO films was approximately 3 times lower than that of the amorphous films. The transmittance of the crystallized films decreased with increasing thickness. Transmittance of the amorphous and crystallized 100-nm-thick ITO films showed about 75 and 83%, respectively, at a wavelength of 550 nm. An attempt to obtain better performances in resistivity, transmittance, and mechanical durability was made by the insertion of an SiO_2 layer onto ITO films. ITO has a refractive index of about 2.0 and it shows a high reflectance for the visible spectrum. In order to decrease the reflectance, an SiO_2 layer that showed a low refractive index (∼1.46) was integrated onto the ITO films. The insertion of an SiO_2 layer between the PET and ITO layers showed a higher durability and a lower resistivity than that of the ITO/PET films.[22] In the present study, SiO_2 layers of various thicknesses were formed onto the ITO/PET and the SiO_2 thickness effect on the resistivity, transmittance, and the mechanical durability of the ITO (100 nm)/PET was investigated in detail. Figure 3a shows the variations in sheet resistance, transmittance, and root mean square (rms) roughness of the SiO_2/ITO (100 nm)/PET as a function of the thickness of SiO_2. The sheet resistance of the SiO_2/ITO/PET was maintained at about 40 Ω/sq. with an SiO_2 layer of 30 nm, indicating no influence from the insertion of the SiO_2 layer. However, the sheet resistance abruptly increased for SiO_2 layers above 50 nm. This result showed that the integration of 30 nm SiO_2 layers did not influence the resistance of the ITO conducting films. Therefore, in the present study,

Downloaded on 2013-09-11 to IP 143.248.118.122 address. Redistribution subject to ECS license or copyright; see ecsdl.org/site/terms_use

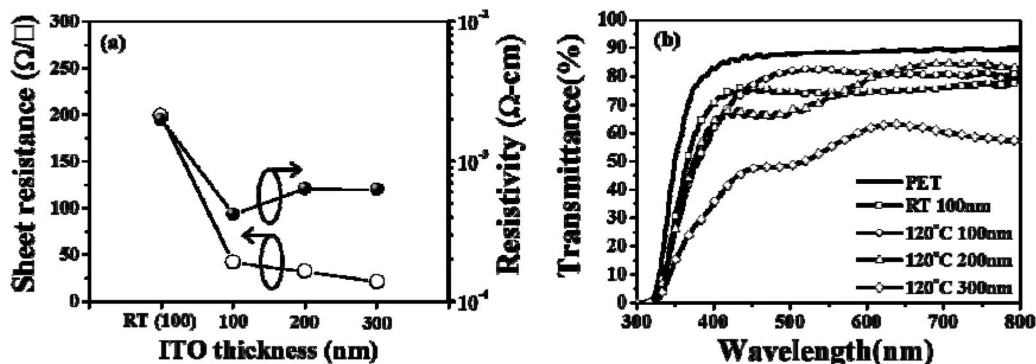

Figure 2. (a) Sheet resistance and resistivity, (b) transmittance of the amorphous and the crystalline ITO films grown onto PET as a function of thickness. Amorphous films were grown at room temperature.

30-nm-thick SiO_2 layers on ITO/PET were noted for an enhancement of transmittance and mechanical durability.

Transmittance of the SiO_2/ITO/PET slightly increased with increasing SiO_2 thickness, showing a maximum of about 87% at an SiO_2 thickness of 50 nm. The effect of the SiO_2 layer on transmittance was definitely shown by the reflective characteristics of the SiO_2 (30 nm)/ITO/PET and ITO/PET (see Fig. 3b). The luminous reflectance values of the SiO_2/ITO/PET and the ITO/PET were approximately 0.7 and 2%, respectively, at a wavelength of 550 nm. A decrease in the reflectance by an SiO_2 layer produced an increase in the transmittance of the SiO_2/ITO/PET. An increase in the SiO_2 thickness slightly increased the roughness of the SiO_2/ITO/PET. Figures 3c and 3d show the reliable durability of the crystallized ITO (100 nm)/PET using a ZrO_2 ceramic ball and a substantial finger touch, respectively. Because the power forced into the films by a ZrO_2 ball was stronger than that of the finger touch, the number of times the finger touch was used was increased to approximate the force of the ZrO_2 ball. Remarkably, the transmittance of the ITO/PET before and after a touch did not vary for either the ZrO_2 ball or the finger touch. In the case of the sheet resistance, films forced by the ZrO_2 ball showed a variation from the 42 Ω/sq. (before touch) to 55 Ω/sq after 300 times, while force by the finger touch showed a variation of 52 Ω/sq. after 500 times. The mechanical durability of the crystallized and amorphous ITO films was tested using only the ZrO_2 ceramic ball and not a finger touch. Figures 4a and 4b show the variations in sheet resistance and the transmittance of the amorphous ITO (*a*-ITO), SiO_2/*a*-ITO, crystallized ITO (*c*-ITO), and SiO_2/*c*-ITO films grown onto PET, respectively, as a function of the number of touches. The 30-nm-thick SiO_2 layer that maintained the resistance of the ITO film and provided the highest transmittance was chosen to investigate the mechanical durability of the SiO_2/ITO/PET. As shown in Fig. 4a, the *c*-ITO films showed an increase in sheet resistance from 42 to

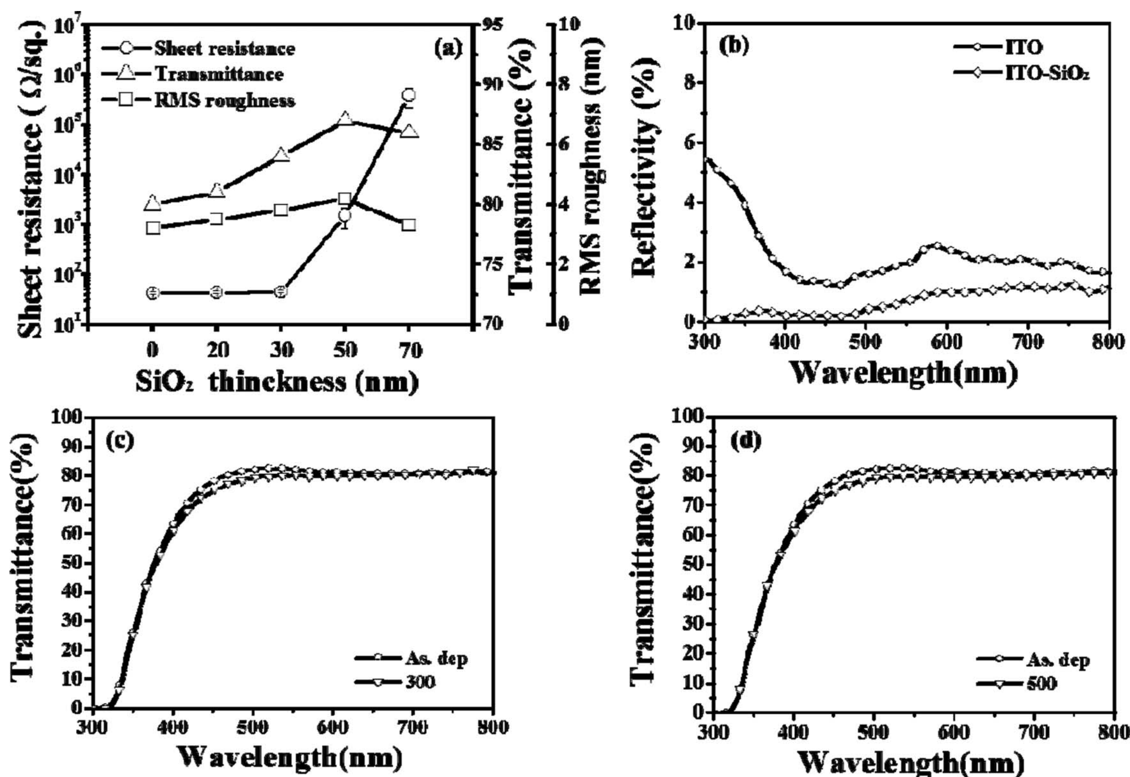

Figure 3. (a) Variations in sheet resistance, transmittance, and root mean square (rms) roughness of the SiO_2/ITO (100 nm)/PET as a function of the thickness of SiO_2. (b) Reflective characteristics of the SiO_2 (30 nm)/ITO/PET and ITO/PET. Transmittance of the 100-nm-thick crystalline ITO films with and without touches using (c) ZrO_2 ceramic ball (300 times) and (d) finger touch (500 times).

Downloaded on 2013-09-11 to IP 143.248.118.122 address. Redistribution subject to ECS license or copyright; see ecsdl.org/site/terms_use

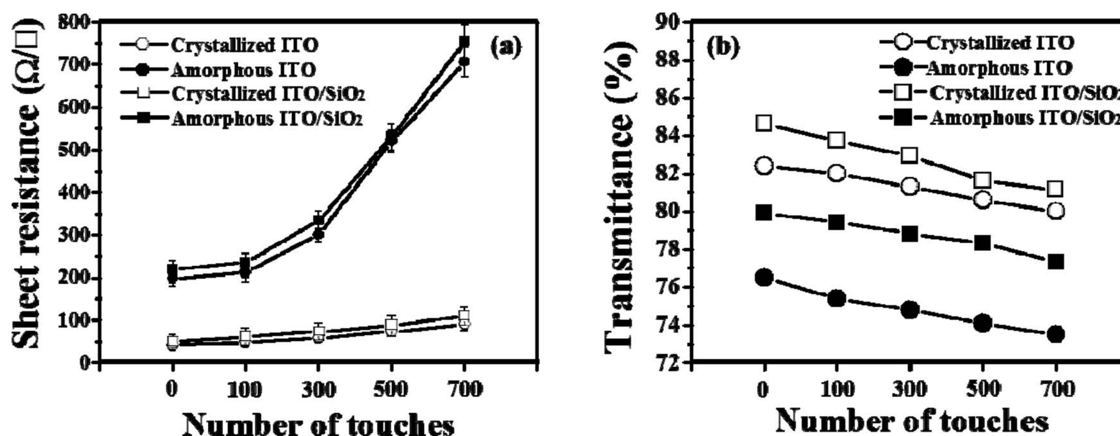

Figure 4. Variations in (a) Sheet resistance and (b) transmittance of the *c*-ITO, *a*-ITO, SiO_2/*c*-ITO, and SiO_2/*a*-ITO films grown onto PET as a function of number of touches.

91 Ω/sq. after touches of 700 times, while the amorphous films showed an abrupt increase in sheet resistance from 200 to 710 Ω/sq. after 700 times. This result suggests that the amorphous films did not exhibit a durability that was acceptable for touch screen applications. Sheet resistances for both the SiO_2(30 nm)/*c*-ITO and SiO_2(30 nm)/*a*-ITO films were slightly increased with an increased number of touches, indicating no effect on the resistance durability after the insertion of the SiO_2 layer compared with no SiO_2 layer. This result suggests that the amorphous SiO_2 did not provide enough mechanical resistance to touches. As shown in Fig. 4b, transmittance of the *a*-ITO films linearly decreased with an increased number of touches and showed a decrease of about 4% after 700 touches, while that of the *c*-ITO films showed a decrease of about 2.5%, maintaining a transmittance of about 80% after 700 touches. The *c*-ITO films showed superior mechanical durability compared with the *a*-ITO films for both resistance and transmittance. A 30-nm-thick SiO_2 layer was integrated onto an amorphous and crystallized 100-nm-thick ITO film and investigated for mechanical durability through variations in transmittance, as shown in Fig. 4b. In the case of both the *c*- and *a*-ITO films, compared with no SiO_2 layer the integration of an SiO_2 layer showed an increase in the absolute transmittance, while the mechanical durability did not show a remarkable effect from the insertion of an SiO_2 layer. Based on the results of mechanical durability testing, the integration of an *a*-SiO_2 layer improved the absolute transmittance of both SiO_2/*a*-ITO and SiO_2/*c*-ITO films, but the mechanical durability was not improved.

Conclusions

The crystallization of ITO films as-grown onto a PET substrate at 120°C was achieved without mechanical damage to the substrate using facial off-axis sputtering. The 100-nm-thick c-ITO films showed a sheet resistance of 42 Ω/square (resistivity: 4.2×10^{-4} Ω-cm) and a transmittance of about 83% at a wavelength of 550 nm. Compared with amorphous ITO films, the crystallized ITO films as-grown onto a PET substrate showed an improved mechanical durability that is necessary for touch-screen applications. The integration of a 30-nm-thick amorphous SiO_2 layer onto ITO/PET maintained the resistivity of the ITO itself and exhibited an improvement in transmittance of about 86% compared with the c-ITO films. The amorphous SiO_2 layer did not impact the mechanical durability of either *a*-ITO or *c*-ITO films grown onto PET.

Acknowledgment

This work was supported by National Research Foundation of Korea (NRL) grant funded by the Korea Government (MEST) (No. 2011-0000359).

References

1. M. R. S. Bulletin, vol. 25, (8) August (2000), *Special Issue on Transparent Conducting Oxides*, Edited by D. S. Ginley 2002.
2. J. W. Elam, D. A. Baker, A. B. F. Martinson, M. J. Pellin, and J. T. Hupp, *J. Phys. Chem. C*, **112**, 1938 (2008).
3. R. B. H. Tahar, T. Ban, Y. Ohya, and Y. Takahashi, *J. Appl. Phys.*, **83**, 2631 (1998).
4. J. Lee, H. Jung, J. Lee, D. Lim, K. Yang, J. Yi, and W. C. Song, *Thin Solid Films*, **516**, 1634 (2008).
5. O. Tuna, Y. Selamet, G. Aygun, and L. Ozyuzer, *J. Phys. D: Appl. Phys*, **43**, 055402 (2010).
6. Y. T. Cheng, J. J. Ho, C. K. Wang, W. Lee, C. C. Lu, B. S. Yau, J. L. Nain, S. H. Chang, C. C. Chang, and K. L. Wang, *Appl. Surf. Sci.*, **256**, 7606 (2010).
7. A. K. Sytchkova, M. L. Grilli, S. Boycheva, and A. Piegari, *Appl. Phys. A*, **89**, 64 (2007).
8. L. Kerkache, A. Layadi, E. Dogheche, and D. Remiens, *J. Phys. D: Appl. Phys.*, **39**, 184 (2006).
9. F. El Akkad, A. Punnoose, and G. Prabu, *Appl. Phys. A*, **71**, 157 (2000).
10. H. M. Ali, H. A. Mohamed, and S. H. Mohamed, *Eur. Phys. J.- Appl. Phys.*, **31**, 87 (2005).
11. C. Liu, T. Mihara, T. Matsutani, T. Asanuma, and M. Kiuchi, *Solid State Commun*, **126**, 509 (2003).
12. F. O. Adurodija, R. Bruning, I. O. Asia, H. Izumi, T. Ishihara, and H. Yoshioka, *Appl. Phys. A*, **81**, 953 (2005).
13. S. V. N. Pammi, N. J. Seong, and S. G. Yoon, *Scripta Mater*, **61**, 867 (2009).
14. S. V. N. Pammi, A. Chanda, N. J. Seong, and S. G. Yoon, *Chem. Phys. Lett.*, **490**, 234 (2010).
15. H. C. Lee and O. O. Park, *Vacuum*, **75**, 275 (2004).
16. W. Deng, T. Ohgi, H. Nejo, and D. Fujita, *Appl. Phys. A*, **72**, 595 (2001).
17. K. Ishibashi, K. Hirata, and N. Hosokawa, *J. Vac. Sci. Technol. A*, **10**, 1718 (1992).
18. Y. Hoshi, H. O. Kato, and K. Funatsu, *Thin Solid Films*, **445**, 245 (2003).
19. K. H. Kim, *J. Ceram. Process. Res.*, **8**, 19 (2007).
20. J. W. Kim et al., "INO 5R Resistive Touch-Screen Specifications", Inotouch Technology Co. Ltd. pp. 1-11, 2003.
21. B. D. Cullity, *Elements of X-ray Diffraction* 2nd edn (Reading, MA; Addision-Wesley), 1978, Chapter 3, p. 102.
22. K. Noda and K. Tanimura, *Electron. Commun. in Jp. Part 2*, **84**, 767 (2001).

Downloaded on 2013-09-11 to IP 143.248.118.122 address. Redistribution subject to ECS license or copyright; see ecsdl.org/site/terms_use